Earth Reinforcement, Ochiai, Yasufuku & Omine (eds) © 1996 Balkema, Rotterdam. ISBN 90 5410 8339

# Reinforced soil failure: Analysis at the biaxial compression test

J.C. Morel & J.P. Gourc
*IRIGM Lgm., University of Grenoble I, France*

ABSTRACT: The plane strain biaxial compression test has an advantage over the triaxial revolution compression test in that it can be used to visualize reinforced soil deformation and enables tests to be conducted for geotextile sheets placed at different angles to the horizontal.

Stereophotogrammetry was used to conduct a detailed analysis of the failure mechanisms and the forces exerted on the reinforcement sheets. After illustrating the block mechanisms involved in failure, with the geotextile sheets breaking, the authors use the experimental results to validate the limiting equilibrium methods generally proposed for this type of problem.

## 1. INTRODUCTION

The results of the present study on the reinforcement of sand by geotextile sheets complement those obtained in a study on micro-reinforcement by micro-grids (Gourc and Morel, 1994). In both cases, the originality of the research derives from the use of a prototype compression apparatus developed by IRIGM, known as "Biaxial". This apparatus enables the sample of reinforced soil to be compressed in two perpendicular directions while maintaining zero deformation in the third direction, perpendicular to the other two (figure 1). The apparatus allows detailed observation of the failure mode in the reinforced soil sample (figure 2).

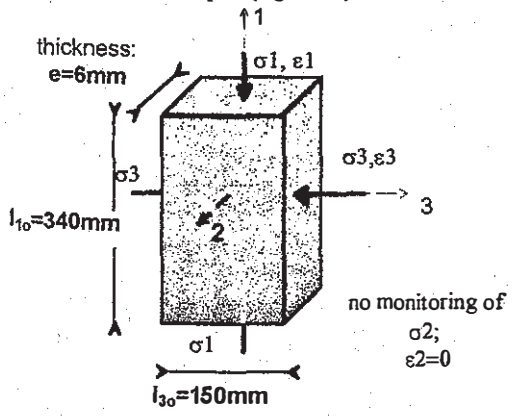


Figure 1 : Size and stress-strain conditions of the biaxial test

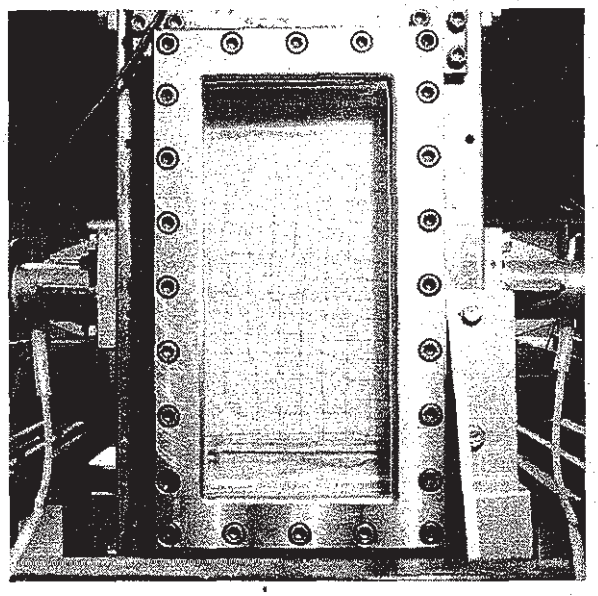

Figure 2 : General view of a sample under compression

## 2. THE BIAXIAL COMPRESSION APPARATUS

IRIGM has developed a special device which differs from the traditional "triaxial" (or axisymmetric triaxial) apparatus used in soil mechanics (Billet and al., 1992). The sample is parallelepipedic and subjected to constant lateral pressure (direction 3, figure 1) by means of rubber bags filled with pressurized water.

Strains are kept constant in perpendicular direction 2. A transparent plate (perpendicular to direction 2) enables continuous monitoring of sample deformation during the compression test, with the strained state of the sample being recorded by a camera. Stereophotogrammetric analysis is used to determine the kinematics and failure mode (displacements, shear strains, volumetric strain field) (Desrues et al., 1985).

In the tests presented, the lateral stress $\sigma 3$ and the vertical displacement rate are constant, but the vertical loading device (two symmetrical jacks) can generate complex stress-strain paths.

## 3. TEST PROGRAMME

With the biaxial test, it is not only possible to show displacements within the sample but also to test the behaviour under compression of soil reinforced by sheets placed at an angle to the horizontal (direction 3). This is not possible with the triaxial test. However, few tests of this type have been reported in the literature (McGown and Andrawes, 1977; Ling and Tatsuoka, 1993). The compression tests presented here, therefore, were conducted on a sample of Hostun sand (Gourc and Morel ,1994), first with no reinforcement, then with geotextile reinforcement. The geotextile used was a non-woven, needle-punched sheet with surface density $\mu$ = 160 g/m$^2$, tensile stiffness J = 30 kN/m and tensile strength $T_f$ = 12 kN/m.

In the reinforced sand, the geotextile sheets were either horizontal (spacing $\Delta H$ = 11.3 cm) or inclined at an angle $\beta = \pm 30°$ to the horizontal (with the same spacing between sheets).

Finally, this series of tests was completed by two tests on sand reinforced by a single sheet placed at angles of $\beta = \pm 50$ and 65°, angles which are close to the orientation of the slip plane of the sand without reinforcement.

## 4. INFLUENCE OF ANGLE OF INCLINATION OF GEOTEXTILE SHEETS ON COMPRESSIVE STRENGTH

All the tests were carried out for the same confining stress $\sigma 3$ = 100 kPa. Figure 3 shows the typical graphs obtained $\sigma 1/\sigma 3 = f(-\varepsilon 1)$ for the reinforced and non-reinforced sand. Additional tests, which are not presented here, were conducted to assess repeatability This was found to be relatively good, even if the shape of the post-peak graphs is unique since, as will be seen later, it is influenced by the failure mode.

A special feature of these graphs is the

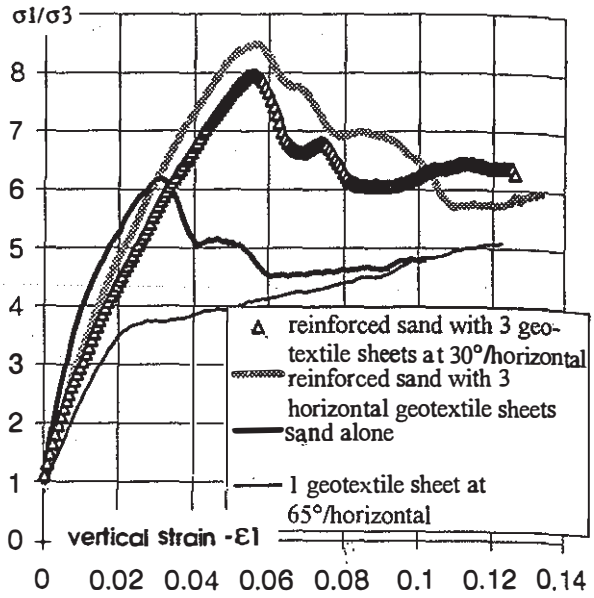


Figure 3 : stress-strain diagram for unreinforced and reinforced sand (by horizontal and inclined geotextile layers)

undulations that appear during the work-hardening phase. This has been observed and explained, in tests on non-reinforced sand, by another author (Desrues et al., 1985).

A significant increase in peak compressive strength is obtained when the soil is reinforced with 3 geotextile sheets. This peak (obtained, as will be seen later, when deformation is localized along a slip line) is obtained for a strain ($-\varepsilon 1$) which is much greater for the reinforced sand than for the non-reinforced sand.

On the other hand, stiffness decreases on account of the geotextile sheets for small strain values. This behaviour may be explained in part by taking into account compressibility, which varies according to geotextile thickness.

Finally, it will be noted that for the maximum experimental strain ($-\varepsilon 1$) = 13% considered for the sand reinforced with three sheets, tensile failure of at least one geotextile sheet occurs. Localised shearing thus takes place in the sand alone, the geotextiles having broken. In spite of this, the compressive strength remains much greater than that observed for sand alone.

In the sand reinforced by a sheet placed at an angle $\beta = \pm 50$ or 65°, a single shear band develops more or less along the geotextile sheet. In this case, the sample has a lower compressive strength for small strain values. On the other hand, compressive strength increases continuously with ($-\varepsilon 1$). This is due to the shear process being disturbed by the geotextile sheet.

## 5. FAILURE KINEMATICS FOR SAND REINFORCED WITH THREE GEOTEXTILE SHEETS

The aim of the present report is to describe how the results of stereophotogrammetry can be used. Equipment at the 3S Laboratory of Grenoble University uses recordings of the displacement of about 200 points on the surface of the sample for successive strain steps of $\varepsilon_1$ to obtain the strain field and to display the failure mode. If the failure mode is known, it is then possible to test the block mechanisms often used to quantify the reinforcement effect.

Observation of the shear strain fields $\frac{\Delta\varepsilon_1 - \Delta\varepsilon_3}{2\Delta\varepsilon_1}$ (distorsion) shows that failure occurs along a shear band at an angle which is more or less independent of the angle of the geotextile sheets, $\beta = \pm 0, \pm 30°$. This angle $\alpha$ varies between 63 and 68°, and corresponds to the sample diagonal and also the angle $\frac{\pi}{4} + \frac{\phi}{2}$ with $\phi_{peak} = 46.1°$ and $\phi_r = 39.5°$.

The localization of deformation (strain concentrations along a shear band and slipping of blocks one on top of the other) appears systematically after the stress peak (figure 4) (Morel, 1996). Figure 4 shows the strain fields for the sand with horizontal geotextile sheets ($\beta = 0$) (test H1) and sheets placed at an angle ($\beta = \pm 30°$) (test I1), calculated from the difference between steps 6 and 7 ($-\varepsilon_1$ varies from 8 to 10%) and between steps 8 and 9 ($-\varepsilon_1$ around 12%). The strain field (S6S7) corresponds to a propagation of the strain area and the field (S8S9) on geotextile failure. The difference between the two strain fields is clear and may be explained in the following way:

- For the horizontal sheets, geotextile failure (figure 5) occurs in the upper sheet in two places which are symmetrical in relation to the vertical axis of symmetry. This breaking of the geotextile is reflected in an increase in slipping along two symmetrical shear bands in the upper part (part which behaves like an element of non-reinforced sand) and in the total disappearance of the diagonal shear band which crosses the lower geotextile sheet (unbroken).

- For inclined sheets ($\beta = \pm 30°$), the main shear band follows the sample diagonal and is accentuated as it runs from (S6S7) to (S8S9), since the central geotextile sheet, intersected by the shear band, is broken in the middle.

The stereophotogrammetric method can thus be used to gain a better understanding of the failure mechanism of a sample of reinforced sand. It should also be noted that failure mechanisms vary from one test to another. For the same type of reinforcement, the resulting shear bands are not systematically the same (figure 8).

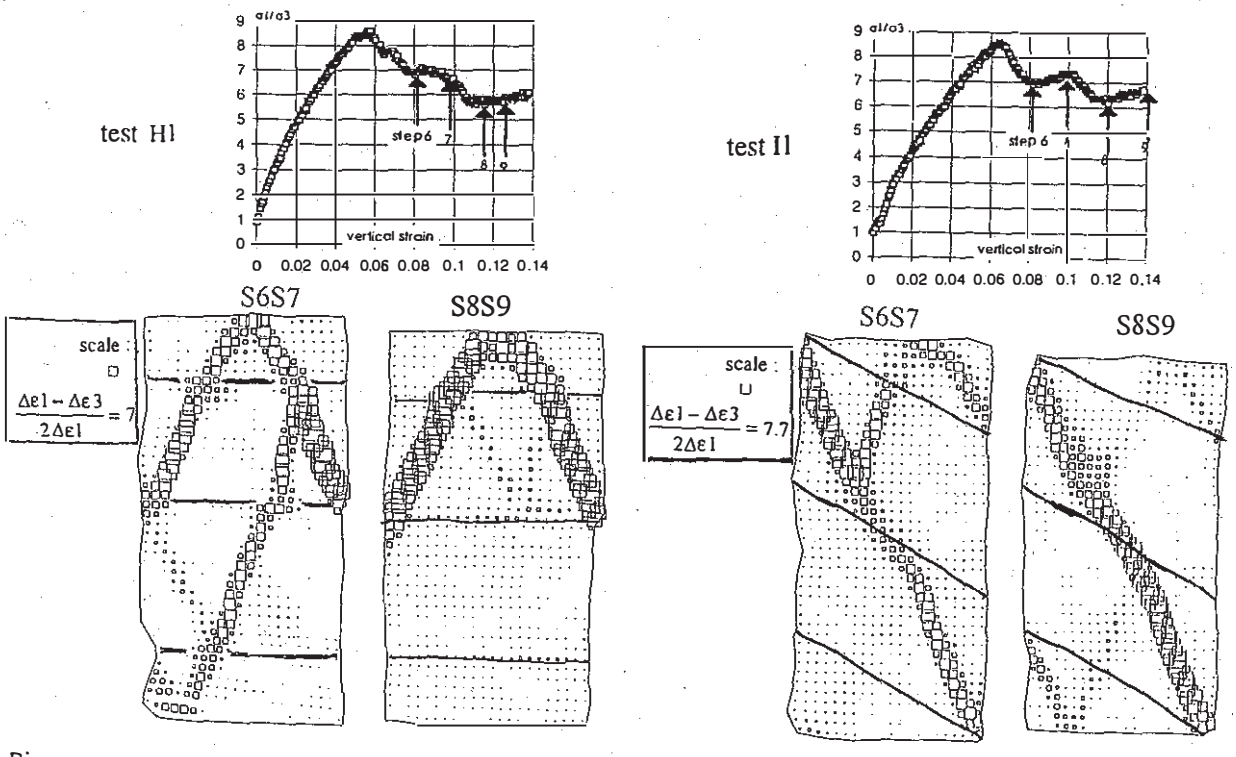


Figure 4 : Sand reinforced by horizontal (H1) or inclined (I1) geotextile layers : distribution of the distorsion rate in the sample

An additional, more detailed, analysis is presented here concerning the soil/geotextile displacements at the interface (figure 6). It helps to clarify the soil/geotextile interaction mechanisms. The case presented corresponds to the sample reinforced by horizontal sheets (S6S7) shown in figure 4. The left-hand drawing represents the displacement vectors, and the block behaviour can be seen again, this time presented in another form. The right-hand drawing represents the relative displacement vectors (sand/geotextile) for the upper and lower interfaces of the geotextiles. Measuring is a delicate process as small marks have to be made and monitored on the geotextile (figure 5). The tangential components of these displacement vectors provide the direction of the tangential stresses induced by the sand on the geotextile and help explain the tensile behaviour of the sheets. At the intersection with the shear bands, it is also possible to show that the sheared geotextile behaves like a membrane.

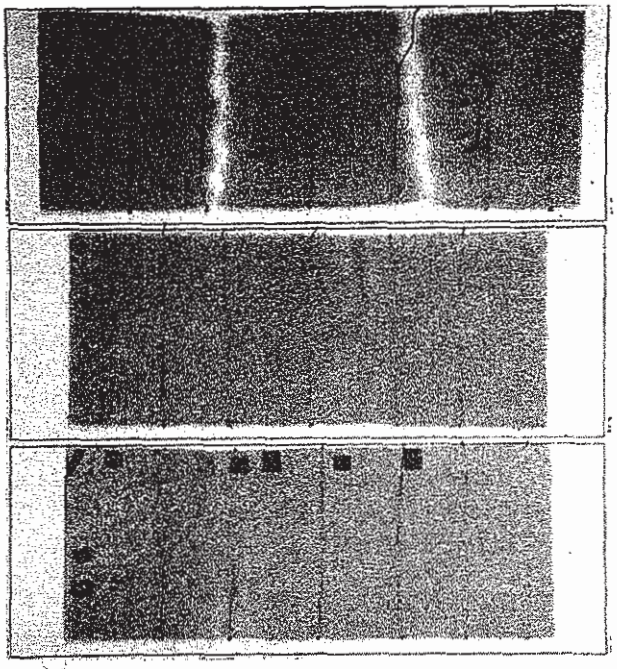

Figure 5 : Geotextile layers at the end of the biaxial compression test (H1)

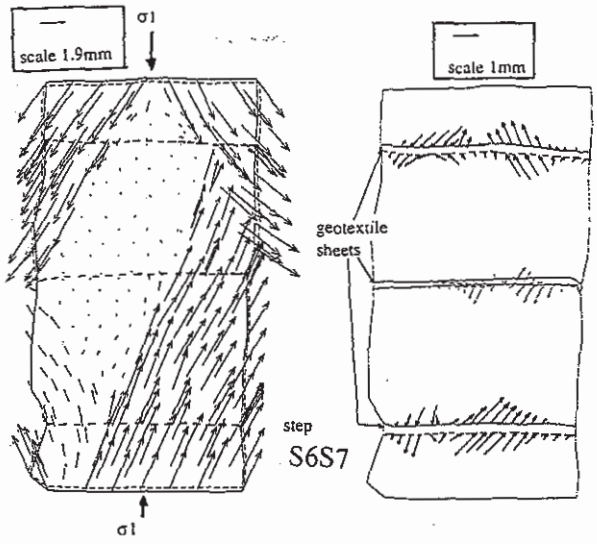


Figure 6 : test (H1) displacements in soil and relative displacements at the interface soil-geotextile

## 6. EVALUATION OF THE REINFORCEMENT EFFECT BY A BLOCK MECHANISM

As shown above, stereophotogrammetry was used to demonstrate a failure in reinforced soil according to a block mechanism, with the application of tensile load and breaking of the geotextiles. The results will now be used to validate the block mechanisms often used to quantify the reinforcement by geotextile sheets in the triaxial compression test or to calculate the stability of retaining structures made of reinforced soil.

The example used is a block of reinforced sand (figure 7) subjected to a stress $\sigma_1$ on its horizontal face, of area $S_0$, and to a stress $\sigma_3$ on its vertical face, of area $S_3$. As indicated above, the shear plane is assumed to be inclined at an angle $\alpha$ to the horizontal. The geotextile sheets (0 to 3) are intersected by this shear plane. These sheets, placed at an angle $\beta$ subjected a tensile load $T_i$ along the shear plane. To facilitate the presentation, the calculation is shown for a shear plane with a fixed

**case a** : the geotextile force direction is along the sheet

geotextile sheet at β

Ti=action of the right block geotextiles sheets on the left block

Rs=action of the right block sand on the left block

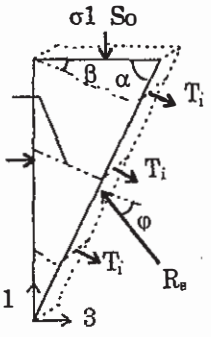


**case b** : the geotextile force direction is along the rupture plane (shear band)

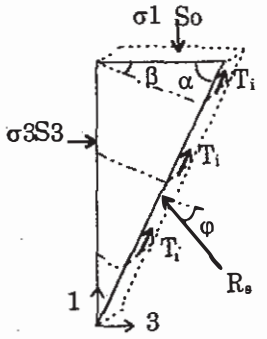


Figure 7 : Mechanism of blocks for reinforced soil

angle $\alpha$, starting from the top right-hand part of the sample. If slip begins at the top left-hand part, instead of taking $(-\alpha)$, an angle $(-\beta)$ was taken for the geotextile sheets and an angle $(+\alpha)$ for the slip plane.

Overall equilibrium is assumed for the block (or two blocks) of horizontal area $S_0$, with applied stress $\sigma_1$ (total width of sample) and n is taken as the number of sheets intersected by the shear band. $R_S$ is the shear strength of the soil along the shear band.

Case a: Direction of tensile loads $T_i$ inclined at $\beta$, tangentially to the initial direction of the geotextile sheets.

Equilibrium in the (1,3) reference frame may be written as follows:

$$/(1)\ \sigma_{1r}.S_0 - R_S.\cos(\alpha-\phi) + n.T_i.\sin\beta = 0$$
$$/(3)\ \sigma_3.S_3 - R_S.\sin(\alpha-\phi) + n.T_i.\cos\beta = 0$$

The following relationship can then be deduced:

$$(a)\ \sigma_{1r} = \frac{\sigma_3 \tan\alpha}{\tan(\alpha-\phi)} + \frac{nTi}{S_0}\left(\frac{\cos\beta}{\tan(\alpha-\phi)} - \sin\beta\right)$$

However, at the intersection with the shear band the geotextile is often found to be subjected to membrane bending. In the extreme case, it may be considered that the geotextile (and the tensile load) is oriented tangentially to the shear band. The new value for $\sigma_1$ is obtained by replacing $\beta$ by $(-\alpha)$.

Case b: tensile load tangential to the shear band

$$(b)\ \sigma_{1r} = \frac{\sigma_3 \tan\alpha}{\tan(\alpha-\phi)} + \frac{nTi}{S_0}\left(\frac{\cos\alpha}{\tan(\alpha-\phi)} + \sin\alpha\right)$$

By way of example, the method for evaluating the reinforcement effect was applied in 4 tests (others are available: Morel, 1996).

In figure 8, the curves have been plotted for $\frac{\sigma_{1r} - \sigma_{10}}{\sigma_3}$ as a function of $\beta$, for cases a and b for an intersection with 1 (n = 1(a) or n = 1(b)), 2 or 3 sheets.

For the 4 tests, two of which are illustrated in Figure 4, the failure modes were represented as follows:

H1: $\beta = 0°$ n = 2 (figures 4 and 5)
H2: $\beta = 0°$ n = 3
I1: $\beta = -30°$ n = 1 (figure 4)
I2: $\beta = +30°$ n = 2

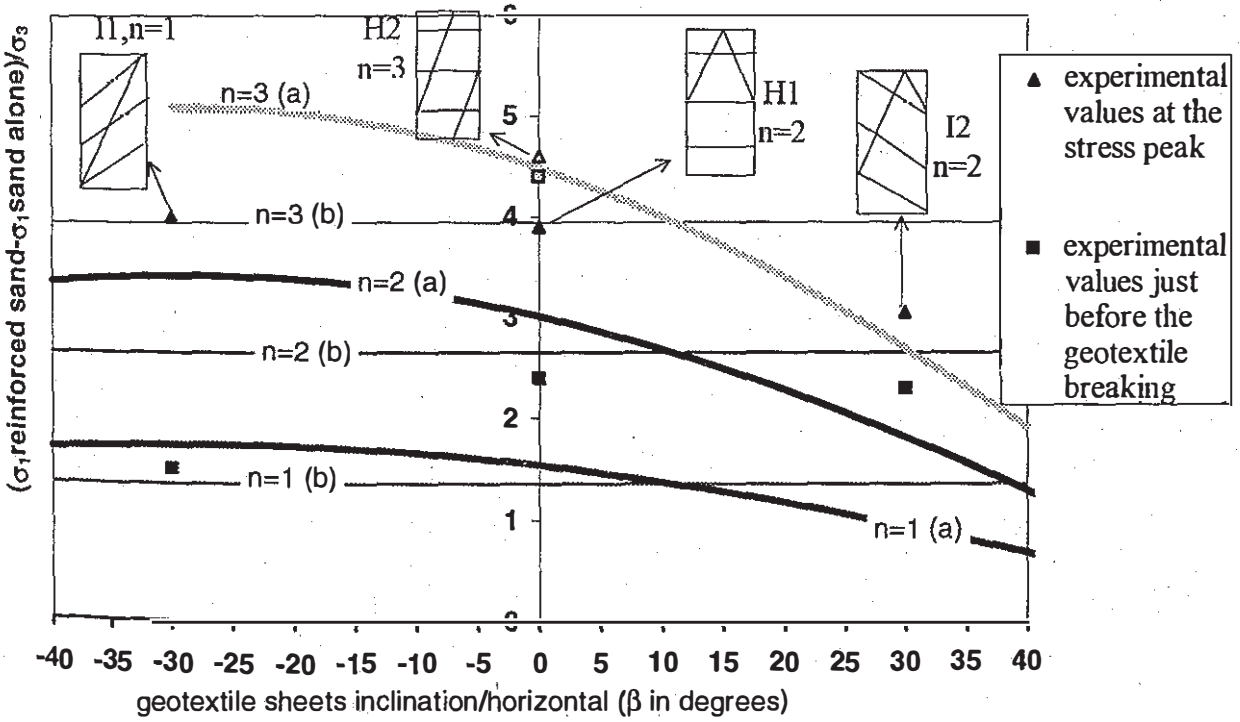


Figure 8 : Comparison between experimental values and theoritical values for the reinforcement effect, for n broken sheets of geotextile

The graphs corresponding to formulations (a) and (b) are plotted for a residual friction angle for the sand of $\phi = 39.5°$, a maximum permissible force in the geotextiles of $T_i = T_f = 12kN/m$, a shear band angle of $\alpha = 68°$, and two values for $\sigma_{1r}$, the first being the stress for a strain $(-\varepsilon_1)$ close to 10 %, just before the geotextile breaks, and the second the stress at the peak.

The most representative experimental values for $\sigma_{1r}$ with respect to the block mechanism are those for 10 % axial strain and not the peak values.

It can be observed that, with the block mechanism, it is possible to come close to the experimental strength values obtained just before the geotextiles break. However, the experimental peak values are much greater. Only the hypothesis whereby the 3 geotextile sheets are subjected to the maximum tensile load would provide a good approximation. This has not yet been verified experimentally.

However, it should be noted that, for test H1, figure 6 indicates that the 3 sheets were subjected to a tensile load and figure 5, which gives a view of the sheets at the end of tests, indicates that all 3 sheets were subjected to a cross-sectional necking as a result of a longitudinal tensile load.

## 7. CONCLUSIONS

By comparison with the equipment used in the standard triaxial compression test, the advantage of the plane strain biaxial compression test apparatus is that it vizualises the deformations of reinforced soil during compression tests and that geotextile sheets placed at different angles to the horizontal can be tested.

The visualization of block rupture mechanisms also made it possible to assess the advantage of limiting equilibrium methods for calculating the strength of reinforced soils. With knowledge of the failure mechanism, the proposed strength for large strains $(-\varepsilon_1 > 10\%)$ was relatively close to the experimental results. For peak strength, the value is close to that obtained by subjecting the 3 geotextile sheets to the maximum tensile load simultaneously.

## REFERENCES


Al Hasani, M.M. 1978. Investigation of strain-stress behaviour of sand tested in plane stain with and without sheet inclusions. *Dissertation submitted for the degree of doctor of philosophy* -University of Strathclyde (scotland)

Billet, P., Gourc, J.P. and Morel, J.C. 1992. Renforcement d'un sable par microgrilles, *Symposium on Textile composite in building construction*, Lyon, partl 147-162.

Desrues, J., Lanier, J. and Stutz, P. 1985. Localization of the deformation in tests on sand sample, *Engineering Fracture Mechanics*, vol. 21, 909-921.

Gourc, J.P., Morel, J.C. 1994. Biaxial compression test on soil micro reinforced by mesh-elements. *5th Intenational conference on geotextiles, geomembranes and related products*, Singapore

Ling, H.I. and Tatsuoka, F. 1993. Laboratory evaluation of a non woven geotextile for reinforcing on-site soil, *Proc. "Geosynthetics 93"*, Vancouver, 533-545.

McGown, A, Andrawes, K.Z. 1977. The influence of non-woven fabric inclusion on the stress strain of a soil mass. *C.R. Coll. Int. Sols Textiles*, Paris, 161-166.

Morel, J.C. 1996. Appareil de compression biaxiale et sol renforcés. *thèse de l'université Joseph Fourier Grenoble I* (in french).